Scilight

Nano-electrochemistry & Nano-photochemistry
https://www.sciltp.com/journals/nenp

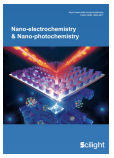

Review

Check for updates

Research Progress and Applications of Enzyme Biofuel Cells in Disease Diagnosis and Treatment

Yang Li [1,†], Shuzhen Yue [2,†], Helena Pardo [3], Zhibin Zhao [1], Lili Zhang [1,*] and Sai Bi [1,*]

[1] College of Chemistry and Chemical Engineering, Shandong Provincial Key Laboratory of Intelligent Molecular Science and Engineering, Key Laboratory of Shandong Provincial Universities for Functional Molecules and Materials, Qingdao Key Laboratory of Intelligent Molecular Manufacturing and Precise Health, Qingdao University, Qingdao 266071, China
[2] Shandong Provincial Key Laboratory of Detection Technology for Tumor Markers, College of Medicine, Linyi University, Linyi 276005, China
[3] Centro NanoMat, DETEMA, Instituto Polo Tecnológico de Pando, Facultad de Química, Universidad de la República, Bypass ruta 8, Pando CAP 9100, Uruguay
* Correspondence: zhanglili2@qdu.edu.cn (L.Z.); bisai11@126.com (S.B.)
† These authors contributed equally to this work.

How To Cite: Li, Y.; Yue, S.; Pardo, H.; et al. Research Progress and Applications of Enzyme Biofuel Cells in Disease Diagnosis and Treatment. *Nano-electrochemistry & Nano-photochemistry* **2026**, *2*(2), 11. https://doi.org/10.53941/nenp.2026.100011

Received: 10 April 2026
Revised: 12 May 2026
Accepted: 14 May 2026
Published: 4 June 2026

Abstract: Detecting and manipulating disease-related bioactive molecules in a controlled way is crucial to elucidate the mechanisms of disease and develop effective diagnostics and therapeutics. Enzymatic biofuel cells (EBFCs) are a kind of fuel cell that rely on enzymes as biocatalysts to convert the chemical energy derived from biosourced fuels into electrical energy. This feature enables EBFCs to be used as self-powered biosensors (SPBs) for biological analysis. This review summarizes the latest research progress in EBFCs in terms of working principles, electron transfer mechanisms, and enzyme immobilization strategies. In addition, it emphasizes applications including disease diagnosis, precision therapy, and theranostic integration. Finally, challenges and opportunities for clinical translation in this field are discussed. By overcoming technical and biological limitations, EBFCs have the potential to revolutionize biomedical diagnostics and therapeutic monitoring, thus fostering the development of efficient and autonomous implantable biosensors.

Keywords: enzymatic biofuel cells; self-powered biosensors; disease diagnosis; precision therapy; theranostics

1. Introduction

The accurate diagnosis and effective treatment of a disease depend on the understanding of its development and pathology. Therefore, accurate molecular detection and intervention of disease-related bioactive species are central to clarifying pathophysiological mechanisms and enabling the rational design of diagnostic and therapeutic strategies [1,2]. In recent decades, stimuli-responsive materials for disease treatment, imaging, and sensing have attracted widespread attention [3]. Among them, driven by continuous progress in nanotechnology, biofuel cells (BFCs) have been recognized as a promising platform for personalized medicine, offering the potential to alleviate the burden on clinical healthcare [4]. BFCs can collect physiological information for long-term, sustained monitoring and therapeutic applications, and provide patients with a comfortable diagnostic experience due to their lightweight and compliant nature [5–8].

BFCs are bioelectrochemical devices that can directly convert chemical energy into electrical energy through electrochemical reactions [9,10]. Among BFCs, enzymatic biofuel cells (EBFCs) represent an important subclass that employs enzymes as biocatalysts to govern fuel oxidation at the anode and oxidants reduction at the cathode. [11]. It is interesting to note that the operating mode of EBFCs is similar to that of the conventional BFCs, while

EBFCs possess significant advantages such as substrate specificity, high energy conversion activity and mild operating conditions [12,13]. These properties allow EBFCs to generate electricity directly from common biological substances like glucose and lactate [14–17]. The electrical energy can be directly used or transformed to other bioavailable energy forms during electron transfer processes [18]. Therefore, EBFCs have dual potential in disease diagnosis and treatment. On one hand, given the quantitative correlation between electrochemical output signals and substrates (such as disease biomarkers), EBFCs can be used as self-powered biosensors (SPBs) for early disease diagnosis [19–22]. On the other hand, EBFCs can provide stable power output to drive implantable medical devices, thus supporting precision therapies, including electrical stimulation and intelligent drug release systems [23–26].

This review outlines the latest progress of EBFCs in disease diagnosis and treatment based. First, we systematically clarify their working principles, electron transfer mechanisms, and enzyme immobilization strategies (Figure 1). Subsequently, we discuss the applications of EBFCs in disease diagnosis, precision therapy, and theranostic integration. Finally, we consider the challenges and prospects for clinical translation in this field, and provide guidance for further research on EBFCs in precision medicine.

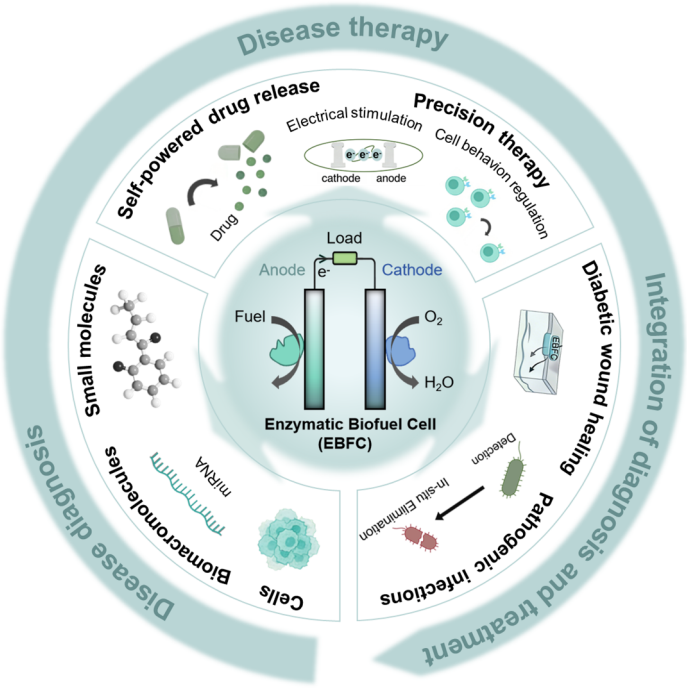

Figure 1. Schematic overview of EBFC-based platforms for disease diagnosis, precision therapy, and theranostic integration.

2. Overview of Enzymatic Biofuel Cells

2.1. Working Principle

The first EBFC concept was proposed by Yahiro et al. in 1964 [27]. They constructed a glucose/oxygen-based EBFC with glucose oxidase (GOD) as the bioanode catalyst and platinum as the cathode catalyst, laying the foundation for subsequent EBFC research. Since then, EBFCs have been developed as a subclass of BFCs, using enzymes as biocatalysts to convert chemical energy into electrical energy under mild conditions [28–31]. The operating principle of EBFCs is similar to that of traditional fuel cells, as both systems convert chemical energy into electrical energy through electrode reactions. However, EBFCs offer clear advantages in terms of cost, fuel renewability, material biodegradability, and biocompatibility, making them particularly attractive for biomedical applications [32]. EBFCs have been designed in various configurations, which differ significantly from traditional fuel cell stacks, to meet the requirements of different application scenarios, but all configurations retain the same core components. These configurations endow EBFCs with broad application prospects in various medical fields, positioning them as an ideal platform for disease diagnosis and treatment [33].

Figure 2 illustrates the working principles of EBFCs. EBFCs adopt a two-electrode system that consists of a bioanode and a biocathode [34]. In EBFCs, natural enzymes are employed as catalysts on the bioanode and biocathode. The bioanode catalyzes fuel (e.g., glucose) oxidation to release electrons. Subsequently, the electrons

flow to the biocathode through an external circuit. The biocathode facilitates the reduction reaction, thereby converting the chemical energy into electrical energy. These EBFCs are powered by endogenous substances, work under mild reaction conditions, and have good biocompatibility and low power consumption [35].

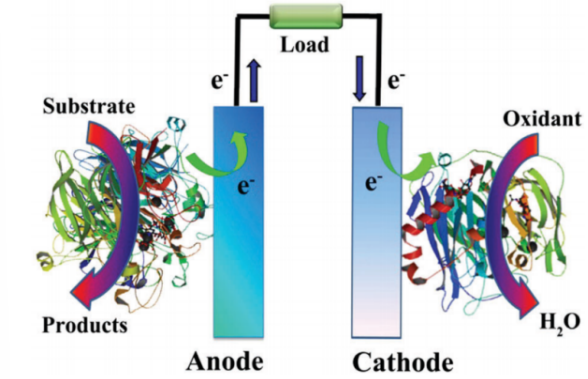

Figure 2. Schematic of a typical EBFC. Reproduced with permission [34]. Copyright 2017, The Royal Society of Chemistry.

2.2. Electron Transfer Mechanism

Efficient energy conversion in EBFCs relies critically on the interfacial electron transfer between biocatalysts and the electrode, which directly determines the power output, energy conversion efficiency, and operational stability of the device [36–38]. Electron transfer mechanisms and pathways depend strongly on the type of biocatalysts employed at the bioanode and biocathode. In this section, we systematically introduce the biocatalysts, the basic electron transfer routes, the enzyme immobilization strategies, and the state of the art progresses of EBFCs.

2.2.1. Biocatalysts

The electron transfer in the bioanode and biocathode of EBFCs is based on oxidoreductases. Oxidoreductases used at the anode include glucose oxidase (GOD), glucose dehydrogenase (GDH), and lactate oxidase (LOx), whose active centers contain coenzymes such as pyrroloquinoline quinone (PQQ) or flavin adenine dinucleotide (FAD) [39–41]. The redox enzymes carry out the oxidation of fuels and produce electrons for electron transfer. At the cathode, the oxidases used within EBFCs are bilirubin oxidase (BOD) and laccase (Lac), and the reaction is catalyzed by multiple copper ions in their active centers. Electrons are supplied from the anode to the oxidases to power the oxygen reduction reaction. Together, the anodic and cathodic enzymes constitute a complete bioelectrocatalytic system for the conversion of chemical energy of fuels into electrical energy [42]. However, the practical EBFC performance is usually restricted by the intrinsic drawbacks of these native oxidoreductases in electron transfer efficiency and catalytic stability.

To improve the catalytic efficiency, researchers have developed a new generation of biocatalysts to overcome the intrinsic limitations of native enzymes in electron transfer efficiency and catalytic stability. First, enzyme engineering has been applied to create high-performance multicopper oxidases (MCOs) with significantly improved electrocatalytic activity. Zhu et al. developed a low-pH-tolerant MCO variant through directed evolution, whose catalytic efficiency was 42-fold higher than that of the original enzyme [11,43]. Second, as an alternative biocatalyst, artificial metalloenzymes (ArMs) comprise abiotic metal cofactors in a protein scaffold. This assembly has been accomplished through multiple strategies, including both covalent and supramolecular anchoring [44]. Bai et al. adopted phase separation techniques to sequester ArMs within membraneless compartments in engineered *E. coli*, which markedly enhanced their stability and catalytic functions, and successfully applied such systems to therapeutic strategies in animal models [45]. In addition to enzyme modification at the molecular level, constructing hybrid architectures by integrating enzymes with conductive nanomaterials has emerged as a powerful strategy to accelerate interfacial electron transfer. These hybrid systems generally involve covalent or supramolecular immobilization of enzymes onto carbon nanotubes, graphene or metal nanoparticles, which act as molecular wires to facilitate electron tunneling between enzyme redox centers and electrode surfaces [46].

2.2.2. Fundamental Electron Transfer Pathways

Electron transfer can be divided into two primary categories: direct electron transfer (DET) and mediated electron transfer (MET) (Figure 3A) [47]. DET is feasible only when the catalytic center or a native electron transfer relay such as hemes lies within the threshold distance for electron tunneling to the electrode [48]. Taking BOD as an example, it harbors four copper atoms, with the trinuclear T2/3 Cu serving as the oxygen reduction site. T1 Cu lies close to the protein surface and communicates with the trinuclear cluster via intramolecular electron transfer, allowing for rapid DET [49,50]. Different from BOD, many enzymes have their active centers deeply embedded within the protein shell, rendering them unable to achieve DET [51]. To address this, mediators are utilized to facilitate electron transfer, a process termed MET. Mediators include methyl viologen, methylene blue, and ferrocene derivatives, which can freely diffuse in solution or be covalently attached to the electrode surface [33,52]. For example, purified GOD from *Aspergillus niger* has its FAD buried at least 1.7 nm from the protein surface, rendering DET impossible. However, some freely diffusing mediators suffer from several disadvantages, such as high cost, potential toxicity, and insufficient stability, which severely restrict their application in implantable and wearable EBFCs.

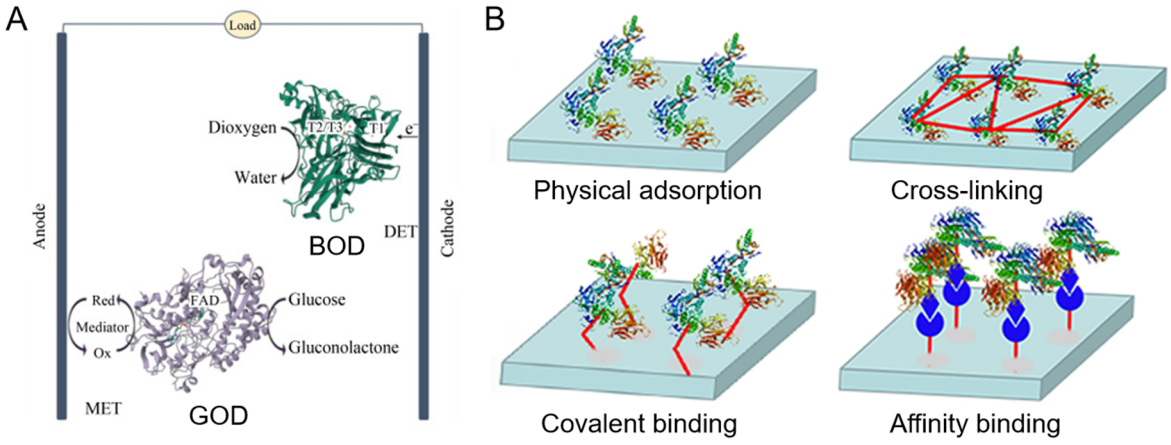

Figure 3. (**A**) Schematic of DET and MET transfer between enzymes and electrodes. Reproduced with permission [47]. Copyright 2021, Wiley-VCH GmbH. (**B**) Schematic of typical enzyme immobilization strategies including physical adsorption, cross-linking, covalent binding and affinity binding. Reproduced with permission [53]. Copyright 2021, Elsevier.

2.3. Enzyme Immobilization Strategies

To overcome the above limitations of DET and MET, several classic optimization approaches have been developed. Among these approaches, enzyme immobilization strategies are the most widely used strategies to facilitate the favorable spatial orientation of enzymes toward the electrode substrate, shorten the distance between the enzyme active center and the electrode, and stabilize the native conformation of enzymes, thus simultaneously improving the electron transfer efficiency of EBFCs [54]. The detailed classification, characteristics, and research progress of enzyme immobilization strategies are systematically elaborated in this section.

Typical enzyme immobilization methods include attachment to solid supports or encapsulation in matrices, which boosts long-term stability, reusability, and operational efficiency. Consequently, the chosen immobilization strategy critically influences the electron transfer efficiency of EBFCs. Enzyme immobilization can be categorized into four main types: physical adsorption, covalent binding, cross-linking, and affinity binding (Figure 3B) [53].

Physical adsorption immobilizes enzymes onto a substrate or matrix via non-covalent interactions, including hydrogen bonding, van der Waals forces, electrostatic forces, and hydrophobic interactions [55,56]. It is a mild and simple method for preserving the native structure of the enzyme without any significant alteration. However, these weak binding interactions often lead to poor long-term stability. On the contrary, the covalent immobilization process is based on the covalent attachment of enzymes to the electrode surface by the formation of covalent bonds between the enzyme functional groups (amino or carboxyl groups) and the active groups of the electrodes [57]. This immobilization method has the advantages of strong binding and high stability, which indicates great potential in enhancing the electron transfer of natural enzymes. However, chemical reactions can change the original structure of enzymes and disturb the enzyme-mediated electron transfer processes. In the case of cross-linking, the use of bifunctional reagents like glutaraldehyde for the formation of a covalent network between enzyme and

support material is also common. This strategy can enhance enzyme retention and stability, but can also cause partial enzyme inactivation, mass-transfer limitations in dense cross-linked networks and increased process complexity. Affinity binding provides a means for controlled enzyme immobilization via specific interactions between affinity tags and their complementary ligands but requires the conjugation of affinity tags (e.g., biotin) onto the enzyme surface [58]. Due to these differences, the choice of an appropriate immobilization strategy should fully consider enzyme performance, electrode material, and intended application to achieve optimal EBFC performance.

2.4. State of the Art of EBFC

Although some progress has been made in EBFCs, their construction still faces significant challenges: first, the catalytic performance of current enzymes is still limited, and continuous efforts are needed to develop enzymes with high catalytic activity [59]. Secondly, the efficiency of electron transfer is limited by the correct orientation between enzymes and electrodes. Although various strategies have been adopted to control the orientation of enzymes on the electrode surface, electron transfer efficiency remains suboptimal. For example, only when the T1 copper center of the enzyme faces the electrode surface, efficient DET be achieved. However, precise control over such orientation with existing methods remains challenging [60]. Third, with the current methods of enzyme immobilization, the spatial distribution of individual enzyme molecules is generally stochastic rather than deterministic, which limits the catalytic efficiency [61].

To address these challenges, the current state of the art focuses on the following frontiers: (1) Using nanostructured electrodes, such as carbon nanotubes, mesoporous gold, graphene, to provide large specific surface areas and shorten electron tunneling distances [62]; (2) Inducing oriented enzyme immobilization via surface chemical modification, such as introducing aromatic groups, carboxyl groups, or enzyme molecular engineering (e.g., site-directed mutagenesis, adding affinity tags) [63]; (3) Developing bifunctional hybrid devices, such as bio-supercapacitors, to compensate for the low instantaneous power density of EBFCs. Nevertheless, achieving long-term stable, efficient EBFCs suitable for implantable medical devices remains a long-term challenge [10].

3. Applications of Enzymatic Biofuel Cells in Disease Diagnosis and Treatment

3.1. Applications in Disease Diagnosis

EBFCs can directly change biomarker concentrations into quantifiable electrical signals, facilitating label-free detection based on the SPB principle without an external power source. The field has developed rapidly since Willner and colleagues first reported an SPB based on EBFCs for glucose and lactate detection in 2001 [64]. Detection targets now range from small molecule metabolites to biomacromolecules and cells. Meanwhile, the sensitivity and functionality of EBFCs have been significantly enhanced. This combination of energy conversion and signal generation renders EBFCs a uniquely powerful platform for disease detection and diagnosis.

3.1.1. Detection of Small Molecule Metabolites

Small-molecule metabolites from human biofluids are attractive biomarkers for clinical diagnosis, prognosis and disease classification due to their linkage to environment, genotype and phenotype [65]. These biosignatures offer a unique metabolic readout, indicating health or disease status and providing important information on downstream products associated with different metabolic pathways. Monitoring and forecasting the dynamic fluctuations of these metabolic biomarkers are needed for systematic, therapeutic, and personalized health management strategies.

For this purpose, Lv et al. fabricated an EBFC using a GOD bioanode and a Lac biocathode, in which bacterial cellulose (BC) electrode modified with carboxylated multi-walled carbon nanotubes (c-MWCNTs) and gold nanoparticles (AuNPs) was employed as the substrate (Figure 4A) [66]. In the EBFC, the large specific surface area of the nanomaterials provided abundant sites for enzyme immobilization, while the conductive network formed by c-MWCNTs and AuNPs significantly enhanced electron transfer efficiency. In recent years, EBFC-SPBs have evolved from standalone devices to integrated and wireless sensing platforms capable of multifunctionality and user-friendly readouts. For instance, Zhang et al. reported a wearable EBFC-SPB system by incorporating EBFCs into diapers to assess glucose levels in diabetic urine [67]. The biosensor was coupled to an energy storage device to power a light-emitting diode (LED). By correlating LED flash frequency with EBFC power output, glucose concentration in the patient's urine could be easily determined [68].

In the context of wearable devices, the printed circuit board (PCB) industry facilitates the rapid and standardized production of electronic circuits, which can be harnessed for electrochemical sensing and fuel cell

applications. For example, Gonzalez-Solino et al. developed the first EBFC on a PCB for self-powered glucose detection in artificial saliva (Figure 4B) [69]. In the EBFC, the PCB gold-plated electrodes were coated with porous gold films to increase the specific surface area. The anode was modified with GOD and an osmium redox polymer mediator, whereas the cathode was modified with BOD and a blocking agent. The resulting EBFC was evaluated in phosphate buffer (PBS) and artificial saliva to confirm its feasibility as a self-powered diagnostic device for use in physiological fluids.

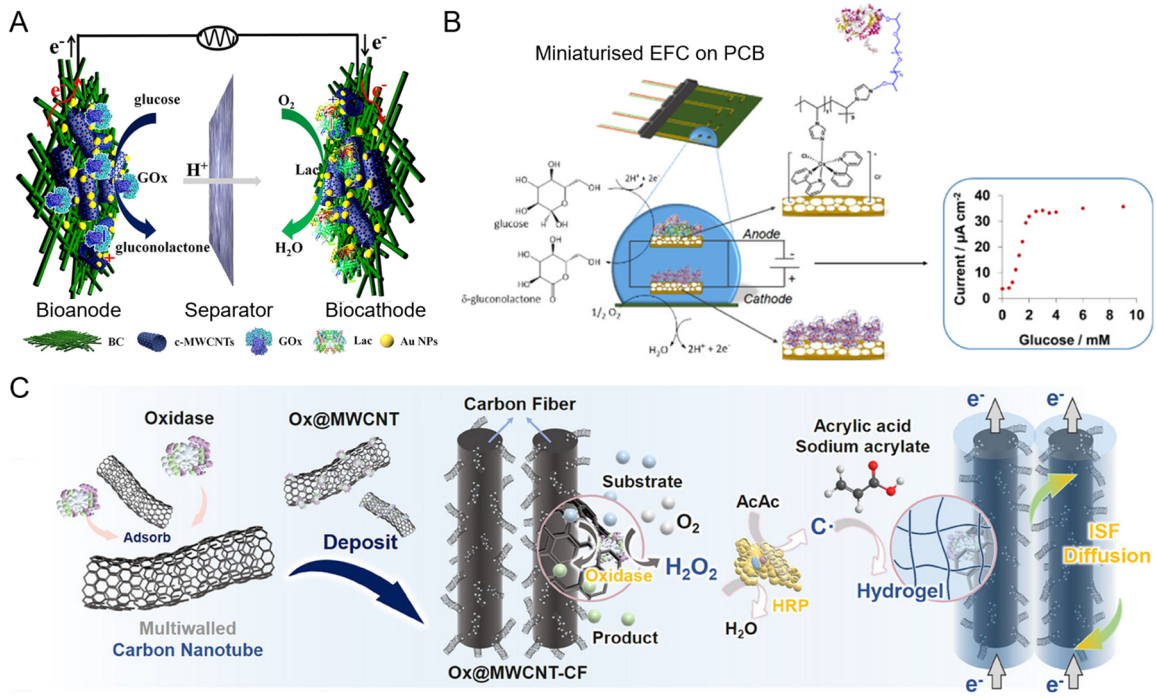

Figure 4. (**A**) Schematic of a flexible EBFC-SPB based on AuNPs-decorated BC. Reproduced with permission [66]. Copyright 2018, Elsevier B.V. (**B**) Schematic of PCB-integrated EBFC for self-powered glucose detection. Reproduced with permission [69]. Copyright 2021, American Chemical Society. (**C**) Schematic of a gel microneedle-based EBFC device. Reproduced with permission [70]. Copyright 2025, Wiley-VCH GmbH.

Additionally, the combination of EBFCs with microneedle arrays and artificial intelligence has expanded their applicability, enabling minimally invasive dynamic monitoring and intelligent prediction. Guo et al. reported a gel microneedle bioelectrode device capable of simultaneously monitoring glucose, lactate, and uric acid in interstitial fluid, with a detection limit for lactate as low as 0.2 mM (Figure 4C) [70]. The device was validated in diabetic rats, enabling accurate detection of metabolic responses to stimuli including exercise and food intake. Furthermore, by integrating data acquisition with an artificial intelligence-assisted analytical system, the device enabled dynamic prediction of biomarkers over the subsequent 20 min. This work represents a major advance toward personalized, responsive healthcare using SPBs.

3.1.2. Detection of Biological Macromolecules

MicroRNAs (miRNAs) and tumor-specific proteins are biomarkers for tumors, genetic diseases, and cardiovascular diseases [71–74]. However, due to their low concentrations in body fluids, conventional EBFC-based SPBs cannot meet the detection requirements. To address this limitation, multiple amplification strategies have been integrated into EBFC platforms for ultrasensitive detection of biological macromolecules. To the best of our knowledge, Gai et al. constructed an EBFC-based self-powered miRNA sensor by integrating a homogeneous electrochemical method, achieving a detection limit of 2.7 aM [75]. This work established a methodological foundation for detecting low-abundance biomacromolecules using EBFC platforms. To further enhance detection sensitivity, Song et al. developed a highly sensitive EBFC-SPB through a capacitor-coupled strategy and DNAzyme-mediated dual strand displacement amplification for miRNA-21 detection in lung cancer [76]. The established detection approach demonstrates great sensitivity, achieving a detection limit of 32.3 aM.

On the basis of single-target detection, Wang et al. developed an EBFC-SPB by integrating catalytic hairpin assembly (CHA), hybridization chain reaction (HCR), capacitors, and a digital multimeter (DMM) for dual-biomarker detection [77]. The biosensor incorporated four components with distinct functions: CHA and HCR for

signal amplification, capacitors (derived from the EBFC) for electrochemical energy storage and conversion, and the DMM for signal readout. The ingenious design enabled a rapid enhancement in the sensitivity of the EBFC-SPB for miRNA detection. This sensor offered ultrasensitive simultaneous quantification of miRNA-21 and miRNA-155, achieving detection limits of 0.15 and 0.66 fM, respectively.

To address the issue of false positives and negatives inherent in single-mode detection, Xu et al. developed a dual-modal EBFC-SPB for the detection of miRNA-141 (Figure 5) [78]. The biosensor was fabricated by the CRISPR/Cas12a cross-cutting technique and a highly efficient nanozyme (AuPtPd@GDY). CRISPR/Cas12a and AuPtPd@GDY were chosen to generate electrochemical and colorimetric signals. The cross-cutting of S2-glucose oxidase (S2-GOD) by CRISPR/Cas12a and the cascade redox reaction of glucose/H_2O_2/TMB lead to electrochemical signal decrease and colorimetric signal increase, respectively, for detecting miRNA-141. Based on this dual-modal SPB system, a smartphone-mediated "all-in-one" biosensing chip was designed to achieve real-time and intelligent monitoring of miRNA-141 in the point-of-care testing (POCT) mode.

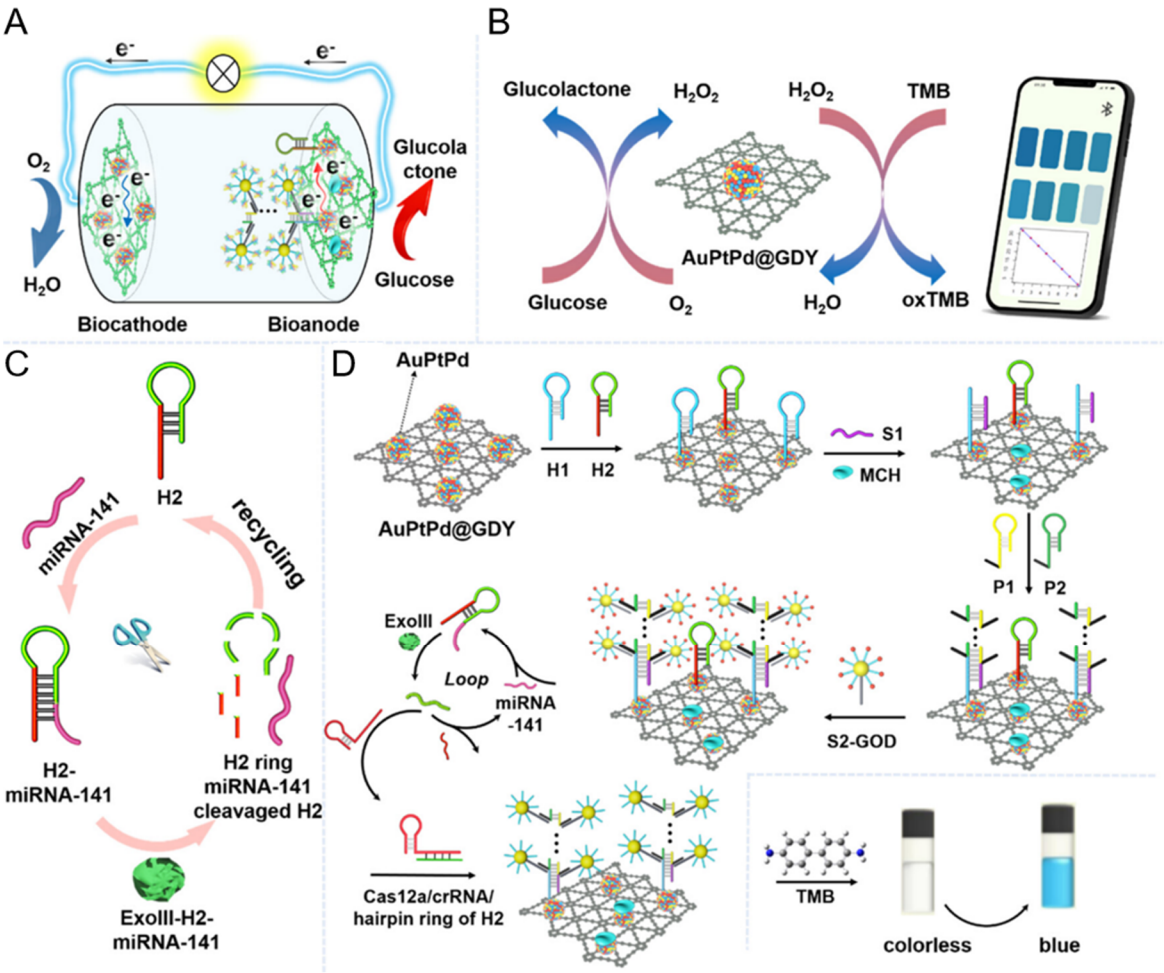

Figure 5. (**A**) Schematic of the dual-modal self-powered EBFC sensing platform. (**B**) Schematic of cascade reaction in the nanozyme system. (**C**) Schematic of the miRNA-141 recycling process. (**D**) Schematic of the electrochemical detection procedure. Reproduced with permission [78]. Copyright 2024, American Chemical Society.

3.1.3. Detection of Tumor Cells

In addition to small molecule metabolites and biological macromolecules, EBFC-SPBs enable the detection of various tumor cells with high specificity and ultrasensitivity by modulating interfacial electrochemical properties through specific recognition and cell capture [79]. For example, Gai et al. constructed a membraneless EBFC-based self-powered cytosensor for cancer cell detection (Figure 6A) [80]. The one-compartment system comprised a biocathode functionalized with BOD-conjugated aptamers and an anode composed of NG/AuNPs/GOD. Upon target cell recognition, the aptamer underwent a conformational change that captured the cells and simultaneously released the BOD conjugate from the cathode surface. The reduced BOD loading impaired the cathodic catalytic activity toward oxygen reduction and decreased the open-circuit voltage, thereby enabling quantitative detection of cancer cells. Building on this design, Gai et al. subsequently developed an

ultrasensitive self-powered cytosensor based on EBFCs to quantitatively detect CCRF-CEM cells. The cytosensor could capture CCRF-CEM cells through Sgc8-mediated receptor-ligand recognition at the cathode, leading to a significant decrease in power output and achieving a detection limit down to 4 cells [81].

Beyond single-target detection and conventional sample processing methods, Yimamumaimaiti et al. designed an EBFC-SPB that integrated a flow cell-supported membrane separation device (FMSC), enabling continuous separation and detection of exosomes (EXOs) and host cells in human serum [82]. In this device, FMSC enabled size-dependent, nondestructive extraction of EXOs. The extracted EXOs and remaining host cells were sequentially introduced into the EBFC-SPB, with the anode and cathode functionalized with different aptamers. The increased steric hindrance resulted in segmental degradation of output performance, thereby enabling dual-target quantification with high sensitivity. This platform provided a powerful tool for analyzing the relationship between EXOs and host cells.

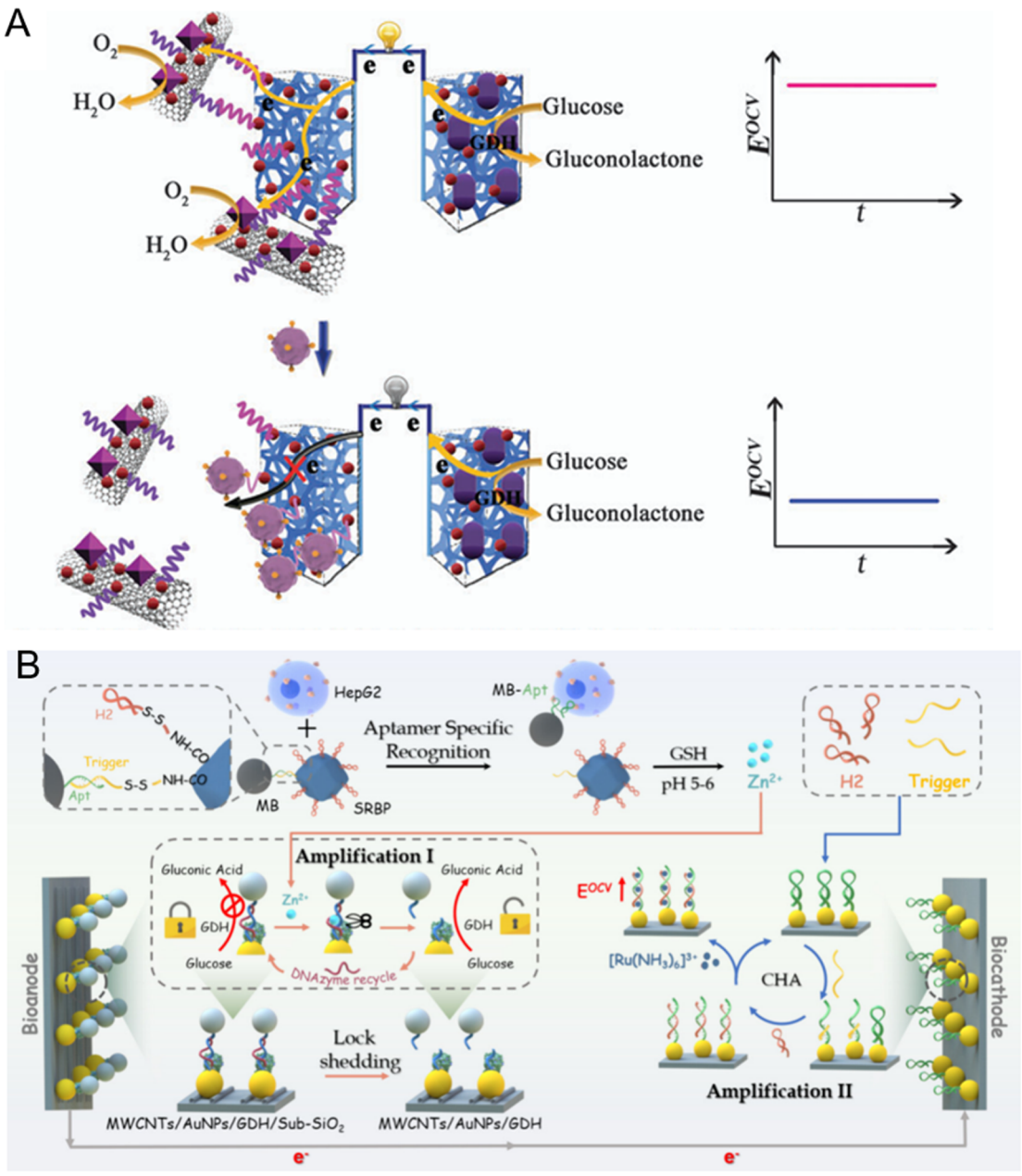

Figure 6. (**A**) Schematic of an EBFC-based self-powered cytosensor. Reproduced with permission [80]. Copyright 2015, The Royal Society of Chemistry. (**B**) Schematic of SRBP-mediated EBFC-SPB with dual-signal amplification for HepG2 CTC detection. Reproduced with permission [83]. Copyright 2025, American Chemical Society.

Circulating tumor cells (CTCs) are critical biomarkers in early cancer diagnosis and prognosis. Among the emerging detection platforms, EBFC-SPBs stand out as powerful for CTC detection. To improve detection sensitivity, Men et al. developed an EBFC-SPB based on a stimuli-responsive barcode probe for recognizing target

HepG2 CTCs, which triggers circuit unlocking and DNA dual-signal amplification for ultrasensitive detection (Figure 6B) [83]. The biosensor has an ultralow detection limit of 3 cells/mL and excellent specificity, which can achieve the ultrasensitive detection of HepG2 CTCs and has great potential for early cancer diagnosis.

To provide an intuitive summary, Table 1 systematically compares representative EBFC platforms for diagnosis in terms of their analytes, EBFC construction, linear range of sensing, LOD of sensing, and other parameters.

Table 1. Representative EBFC platforms for diagnosis.

Analytes	EBFC Construction	Linear Range of Sensing	LOD of Sensing	Others	Ref.
Glucose	Anode: BC/c-MWCNTs/AuNPs-GOD; Cathode: BC/c-MWCNTs/AuNPs-Lac	0–50 mM	2.874 μM	Peak power density: 345.14 μW cm^{-3}	[66]
Glucose (in urine)	Anode: CNTs/AuNPs-GOD; Cathode: MnO_2/CNTs	1–5 mM	1 mM	Peak power density: 220 μW cm^{-2} (in 5 mM glucose)	[67]
Glucose (in PBS/artificial saliva)	Anode: GOD/Os/hPG/Au; Cathode: SB/BOD/hPG/Au	PBS: 50 μM–1 mM; Artificial saliva: 0.75–2 mM	PBS: 50 μM; Artificial saliva: —	Peak power density: 9.6 ± 1.4 μW cm^{-2} (in 6 mM glucose)	[69]
Glucose, lactic acid, uric acid	Anode for glucose detection: GOD@MWCNT-CF; Anode for lactic acid detection: LOx@MWCNT-CF; Anode for uric acid detection: UOx@MWCNT-CF; Cathode: BOD@MWCNT-CF	Glucose: 0–12.0 mM; Lactic acid: 0.4–20 mM; Uric acid: 0.1–0.8 mM	Glucose: 0.2 mM; Lactic acid: 0.2 mM; Uric acid: 0.05 mM	Peak power density: 1.98 mW cm^{-2} (20 mM glucose)	[70]
miRNA-21	Anode: GOD/CNT/AuNPs/ITO; Cathode: ITO with $[Fe(CN)_6]^{3-}$ encapsulated in csDNA-capped PMSN	0.01–1 × 10^3 fM	2.7 aM	$E^{OCV} = 0.511 + 0.027 \log C$ ($R^2 = 0.9946$)	[75]
miRNA-21	Anode: GOD/AuNPs/GDY/CP; Cathode: HCR product/AuNPs/GDY/CP	0.1 fM–10 nM	32.3 aM	$E^{OCV} = -0.0293 \log C + 0.5047$ ($R^2 = 0.997$)	[76]
miRNA-21 and miRNA-155	Anode: GOD/AuNPs/CP; Cathode for miRNA-21 detection: H4, H3/H2/H1/AuNPs/CP; Cathode for miRNA-155 detection: miRNA-155/H1/AuNPs/CP	miRNA-21: 0.1–1 × 10^4 fM; miRNA-155: 1–1 × 10^4 fM	miRNA-21: 0.15 fM; miRNA-155: 0.66 fM	miRNA-21: $E^{OCV} = 0.04637 \log C + 0.7617$ (R = 0.996); miRNA-155: $E^{OCV} = -0.03925 \log C - 0.3999$ (R = 0.994)	[77]
miRNA-141	Anode: CRISPR/Cas12a-crRNA/ExoIII-miRNA-141/S2-GOD/P1-P2/S1/H1-H2/AuPtPd@GDY/CP; Cathode: BOD/AuPtPd@GDY/CP	Electrochemical detection: 0.01–1 × 10^5 fM; Colorimetric detection: 0.05–1 × 10^6 fM	Electrochemical detection: 3.1 aM; Colorimetric detection: 15 aM	$E^{OCV} = -0.0675 \log C - 0.57$ ($R^2 = 0.997$)	[78]
miRNA let-7a	Anode: Zn bar; Cathode: PDTB/Au NPs/H1/MCH + S2 + MOFs@GOD-H2/ITO	10 fM–10 nM	1.38 fM	Peak power density: 22.8 μW cm^{-2}	[79]
CCRF-CEM cells; MCF-7 cells	Anode: G/CNT/AuNP/PQQ-GDH; Cathode for CCRF-CEM cell detection: BOD-bioconjugate/Apt_{Sgc8c}/G/CNT/AuNP; Cathode for MCF-7 cell detection: BOD-bioconjugate/Apt_{SYL3C}/G/CNT/AuNP	5–5 × 10^4 cells (both lines)	CCRF-CEM cells: 3 cells; MCF-7 cells: 2 cells	CCRF-CEM cells: $E^{OCV} = 0.529 - 0.040 \log N_{cells}$ ($R^2 = 0.9994$); MCF-7 cells: $E^{OCV} = 0.523 - 0.059 \log N_{cells}$ ($R^2 = 0.9954$)	[80]
EXOs from HeLa cells; HeLa cells	Anode: GDL/SWCNTs/AuNPs/GOD/Apt_{CD63} Cathode: GDL/SWCNTs/AuNPs/BOD/Apt_{MUC1}	EXOs: 10^3–10^7 particles/mL; HeLa cells: 5–5 × 10^4 cells/mL	EXOs: 5.59 × 10^3 particles/mL; HeLa cells: 25 cells/mL	$\Delta P^{cells} = 2.5906 + 4.6893 \log N_{cells}$; $\Delta P^{EXOs} = 6.3836 \log N_{EXOs} - 14.0578$ ($R^2 = 0.98$)	[82]
HepG2 CTC	Anode: GDH/MWCNTs/PDDA/AuNPs/Sub-SiO_2/DNAzyme on FTO; Cathode: AuNPs/H1 on FTO	50–10^6 cells/mL	3 cells/mL	$E^{OCV} = -0.0005 + 0.028 \log C$ ($R^2 = 0.995$)	[83]

Abbreviations: Apt, aptamer; AuNPs, gold nanoparticles; BC, bacterial cellulose; BOD, bilirubin oxidase; c-MWCNTs, carboxylated multi-walled carbon nanotubes; CF, carbon fiber; CNT, carbon nanotube; CNTs, carbon nanotubes; CP, carbon paper; crRNA, CRISPR RNA; CTC, circulating tumor cell; ExoIII, exonuclease III; EXOs, exosomes; FTO, fluorine-doped tin oxide; G, graphene; GDH, glucose dehydrogenase; GDL, gas diffusion layer; GDY, graphdiyne; GOD, glucose oxidase; HCR, hybridization chain reaction; hPG, highly porous gold; ITO, indium tin oxide; Lac, Laccase; LOD, limit of detection; LOx, lactate oxidase; MCH, 6-mercapto-1-hexanol; MnO_2, manganese dioxide; MOFs, metal-organic frameworks; MWCNT, multi-walled carbon nanotubes; Os, osmium polymer; PBS, phosphate-buffered saline; PDDA, poly(diallyldimethylammonium chloride); PDTB, poly(1,4-di(2-thienyl))benzene; PMSN, positively charged mesoporous silica nanoparticles; PQQ-GDH, pyrroloquinoline quinone-dependent glucose dehydrogenase; SB, StartingBlock; Sub-SiO_2, substrate-linked SiO_2; SWCNTs, Single-walled carbon nanotube; UOx, uric acid oxidase. All metrics sourced from primary source abstracts or full text; no value included that could not be independently verified.

3.2. Therapeutic Applications

In addition to disease diagnosis, EBFCs offer self-powered platforms that enable therapeutic applications. The disease treatment applications include self-powered drug release, precision therapy and theranostic integration.

3.2.1. Self-Powered Drug Release

Self-powered drug release represents a key therapeutic application of EBFCs, in which the electrical energy generated by the biofuel cell is utilized to drive therapeutic agent delivery without an external power supply [84–86]. For example, Ogawa et al. developed an iontophoresis patch driven by a built-in EBFC (Figure 7A) [87]. The EBFC comprised enzyme electrodes, a poly(3,4-ethylenedioxythiophene)/polyurethane (PEDOT/PU) resistor, and fructose fuel-loaded hydrogel sheets and chemical drugs. The patch could generate a transdermal ionic current through a fructose-driven electrochemical reaction. The current flowed from the bioanode to the biocathode, thereby facilitating the release of chemical drugs from the hydrogel into the skin.

Subsequently, Xiao et al. achieved a breakthrough in controllable release by developing an EBFC for in situ drug delivery in cell culture media (Figure 7B) [88]. The EBFC was prepared using an osmium redox polymer-mediated GOD-loaded anode and an osmium redox polymer-mediated BOD/drugs-encapsulated cathode. Under closed-circuit conditions with glucose and O_2, redox reactions altered polymer–drug electrostatic interactions, triggering drug release. Different from earlier continuous release systems, this EBFC enabled temporal control, highlighting the promise of self-powered drug release platforms for implantable applications.

To translate these concepts into practical wearable therapeutics, Li et al. developed an EBFC-powered facial mask on non-woven fabric for iontophoresis-facilitated transdermal drug delivery (Figure 7C) [89]. Its performance in EBFC-powered iontophoresis was then demonstrated. The integrated device promoted transdermal delivery of multiple tested molecules, representing a step toward consumer-oriented self-powered drug delivery.

The therapeutic applications of EBFCs have been extended from drug release in solution systems to transdermal drug delivery [90,91]. Guan et al. proposed an EBFC to penetrate the stratum corneum and deliver large drug molecules (Figure 7D) [92]. The biofuel cell comprised a microneedle patch, a Pt/C cathode, and an MXene/CNT/GOD bioanode, with glucose from interstitial fluid and oxygen from ambient air. After the patch penetrated the stratum corneum to access interstitial fluid, glucose in the fluid gradually diffused to the MXene/CNT/GOD bioanode surface and was oxidized for the production of electrons, gluconolactone (GDL), and hydrogen ions. Concurrently, the charged drugs preloaded in the microneedle was released into the dermal layer.

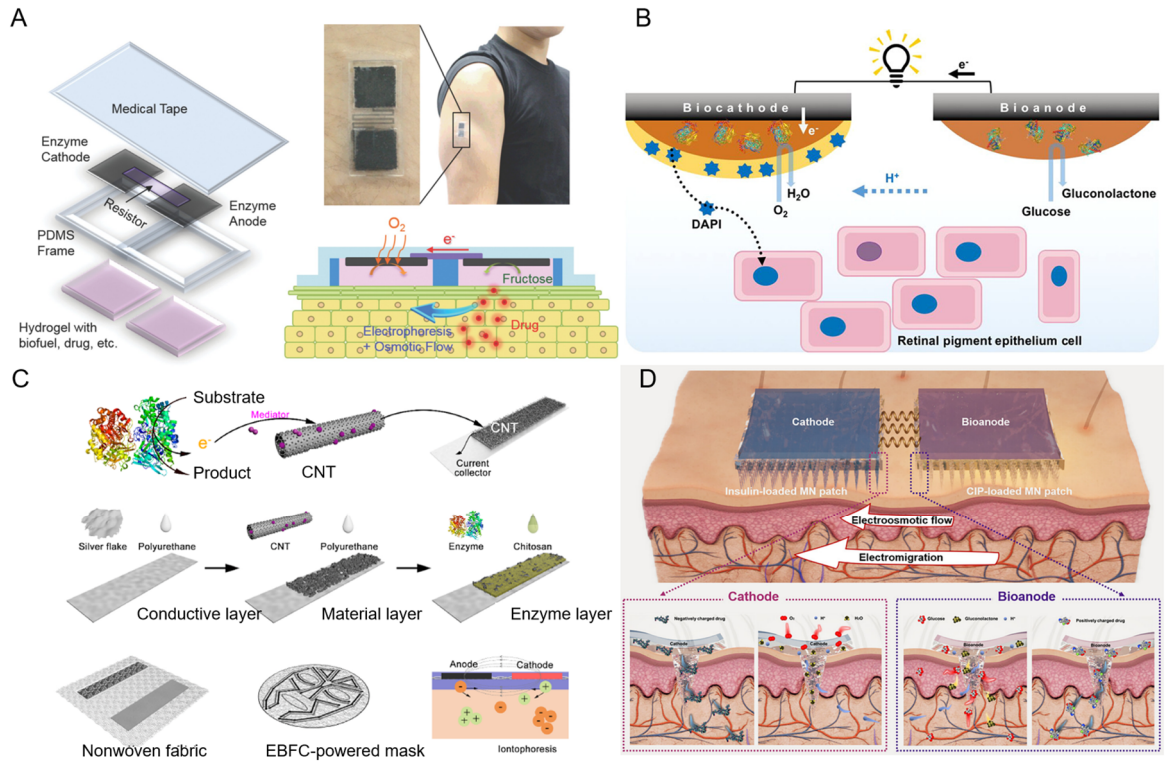

Figure 7. (**A**) Schematic of composition and working principle of fructose/O_2 EBFC-based transdermal iontophoresis patch [87]. Copyright 2015, Wiley-VCH GmbH. (**B**) Schematic of the self-powered release of DAPI

based on an EBFC in a cell culture medium. Reproduced with permission [88]. Copyright 2020, American Chemical Society. (**C**) Schematic of preparation of the EBFC-powered iontophoretic facial mask. Reproduced with permission [89]. Copyright 2022, Elsevier B.V. (D) Schematic of working principle of microneedle-based EBFC. Reproduced with permission [92]. Copyright 2025, Wiley-VCH GmbH.

3.2.2. Precision Therapy

Asymmetric ion channels in epithelial cells transport cations to the basal side and anions to the apical side, generating a transepithelial potential. Upon injury, a wound current flows outward, creating a lateral electric field with the wound edge as the anode and the center as the cathode. Electrical stimulation can effectively regulate the lateral electric field, thereby accelerating tissue repair and wound healing [93]. Inspired by this discovery, Lee et al. first utilized an EBFC to mimic natural electrical stimulation for tissue regeneration. They found that EBFC-generated electrical stimuli could upregulate the expression of myogenic markers and promote the proliferation, migration and myotube formation of muscle precursor cells, demonstrating the potential of EBFCs in wound healing [94]. Building on this concept, Kai et al. fabricated a stretchable bioelectric plaster by incorporating a built-in fructose/O_2 EBFC that conformed dynamically to the skin and generated ionic current along the skin surface for over 12 h (Figure 8A) [95]. Animal experiments confirmed that the ionic current produced by the EBFC significantly enhanced the migration of keratinocytes and fibroblasts toward the wound during the proliferative phase, providing the first *in vivo* proof-of-concept for EBFC-based electrical stimulation therapy. Subsequently, Kim et al. revealed that the microcurrent generated by an EBFC-based skin patch activated the mechanosensitive ion channel Piezo1 to mediate Ca^{2+} influx, thereby regulating the functions of fibroblasts and endothelial cells. This regulation further stimulated cell viability, migration, angiogenesis, collagen deposition, and re-epithelialization, ultimately accelerating wound closure [96]. The above findings support EBFC-based skin patches as a self-powered platform to create self-generating biomedical materials or devices applicable to tissue healing and repair.

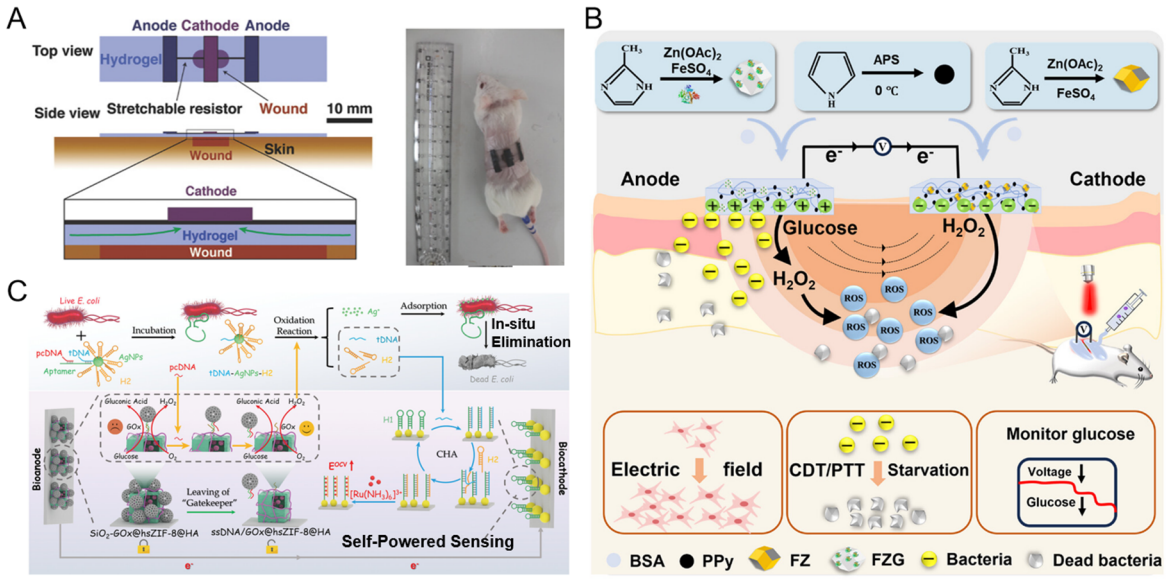

Figure 8. (**A**) Schematic and photograph of the EBFC-based bioelectric plaster for skin wound treatment. Reproduced with permission [95]. Copyright 2017, Wiley-VCH GmbH. (**B**) Schematic of the self-powered EBFC for synergistic therapy and real-time monitoring of diabetic wounds. Reproduced with permission [97]. Copyright 2026, Wiley-VCH GmbH. (**C**) Schematic of the EBFC-SPB integrated with hollow MOF nanoreactors and CHA amplification for *E. coli* detection and in situ elimination. Reproduced with permission [98]. Copyright 2025, Wiley-VCH GmbH.

Beyond drug delivery and electrical stimulation therapy, EBFCs enable precise regulation of cell behavior at the molecular level, providing a new strategy for non-genetic intervention of cell function. For instance, Geng et al. developed a membraneless, EBFC-based self-powered platform for Zn^{2+}-mediated cell membrane receptor reprogramming, which enabled precise control over cell proliferation and migration [99]. This "sensing-actuating-treating" platform enables chemical regulation of cellular behaviors, holding great promise for precision biomedicine.

Despite this promise, EBFC-based systems exhibit distinct merits and inherent limitations when compared with conventional therapeutic strategies. Unlike battery-powered implants, EBFCs utilize endogenous biofuels to

enable self-sustained operation, circumventing issues of limited battery capacity, frequent replacement or recharging, and biosafety risks associated with conventional implantable batteries [46,100]. Compared to conventional transdermal delivery that suffers from inefficient passive diffusion and poor controllability, EBFCs enhance permeability via iontophoresis, enabling active and controllable drug administration [89]. In contrast to systemic administration, they integrate on-site electricity generation with targeted delivery to achieve localized intervention and reduce off-target toxicity [88]. However, critical bottlenecks remain for clinical translation. First, unlike nanomedicines that reach deep organs via the enhanced permeability and retention effect, EBFCs mainly exist as patches, microneedles, and subcutaneous implants that depend on surface oxygen and fuel supply, preventing adaptation to deep-tissue microenvironments. Second, their power output is constrained by sluggish enzyme kinetics, low electron transfer efficiency, and limited enzyme loading, yielding only microwatt-to-low-milliwatt power that is insufficient for clinical electrotherapy requirements. Third, systematic long-term *in vivo* biosafety and biocompatibility assessments, as well as unified clinical evaluation protocols, are still lacking.

3.3. Integration of Diagnosis and Treatment

Self-powered systems that integrate diagnosis, therapy, and evaluation are gaining interest for cancer treatment, particularly in real-time monitoring of therapeutic responses [101–103]. A representative example of such a multifunctional platform is the autonomous "sense-act-treat" system developed by Zhou et al. [104]. The system consisted of a logic-controlled enzymatic anode and a conducting polymer (CP) cathode functionalized with a drug. By employing Boolean AND logic at the anode, the system enabled logic-controlled power output from EBFCs, triggering therapeutic intervention upon detecting abnormal conditions. Furthermore, Wang et al. developed a self-powered platform based on a glucose/O_2 fuel cell [105]. This platform established a complete "diagnosis-therapy-evaluation" closed-loop system by enabling miRNA-triggered diagnosis and targeted drug release at the anode, while capturing apoptotic cells at the cathode for real-time therapy response evaluation. It represents a promising platform for providing valuable information to clinical cancer therapy.

Addressing the clinical management challenges of diabetic wounds, Deng et al. developed a self-powered EBFC using protein hydrogel patch electrodes to achieve synergistic therapy and real-time monitoring of diabetic wounds (Figure 8B) [97]. To construct the patches, zeolitic imidazolate framework-8 (ZIF-8) and its glucose oxidase-loaded form were respectively integrated into a bovine serum albumin (BSA)/polypyrrole (PPy) electrode scaffold. BSA provided structural support for the hydrogel, and PPy endowed the hydrogel with photothermal and conductive properties. The anode regulated the wound microenvironment by consuming glucose to generate reactive oxygen species (ROS), which worked synergistically with near-infrared (NIR) heat to achieve precise sterilization. The microelectric field generated between electrodes accelerated cell migration via electrical stimulation, promoting wound healing. Meanwhile, the electrical signal from the EBFC's glucose-consuming enzymatic reaction correlated with glucose concentration, allowing real-time quantitative monitoring of local glucose levels for diagnosis and treatment.

Beyond cancer treatment, self-powered platforms have also been explored for diagnosis and treatment of pathogenic infections. For example, Wang et al. reported a self-powered platform for highly sensitive detection and in situ elimination of *Escherichia coli (E. coli)* (Figure 8C) [98]. They synthesized hollow porous metal-organic frameworks (MOFs) to harbor GOD for bioanode modification, thereby improving enzyme activity and stability in practical applications. Meanwhile, they designed an aptamer for recognition of the target *E. coli* and employed CHA on the biocathode to amplify signals. This study presents a novel strategy to simultaneously detect and in situ eliminate pathogenic environmental bacteria.

4. Conclusions and Outlook

This review briefly summarizes recent progress on the working principles, electron transfer mechanisms and enzyme immobilization strategies of EBFCs, and systematically reviews their applications in diagnosis, therapy and theranostic integration. EBFCs are a promising platform for disease diagnostics and therapy due to their inherent advantages such as naturally sourced fuel, mild operating conditions, excellent biocompatibility, self-powered capability, and miniaturization.

Despite major advances in EBFCs, several critical challenges remain to be addressed to enable their practical applications. The first challenge is insufficient power output. Due to low electron transfer efficiency at the enzyme-electrode interface, hindered mass transport, and limited electroactive surface area of conventional electrode materials, EBFCs usually exhibit insufficient power output [11]. The second challenge is poor long-term operational stability. Due to the intrinsic structural and catalytic instability of natural enzymes, the inherent performance trade-off of enzyme immobilization strategies, and non-specific biofouling of the electrode surface

in complex biological fluids, EBFCs exhibit poor long-term stability, resulting in rapid performance decay that prevents their use in chronic or implantable applications [14]. The third challenge is unresolved biosafety concerns. The poorly defined biosafety profiles of emerging electrode materials, together with the lack of systematic long-term in vivo biocompatibility assessments and standardized performance evaluation protocols, collectively hinder the practical deployment of EBFC technology.

Against the backdrop of the above challenges, future research may make breakthroughs in several directions: (1) Development of advanced nanomaterials (e.g., graphene, carbon nanotubes, MOFs) [106,107]. Due to their high conductivity and large surface area, these materials can load abundant enzymes and promote efficient electron transfer. In addition, surface functionalization and hierarchically porous structures of these advanced nanomaterials are expected to be promising approaches to further improve enzyme immobilization and stabilization to increase activity retention and energy conversion efficiency [108]. (2) Power management strategies. The voltage and power output of a single EBFC are insufficient. Voltage boost circuits or multi-cell series configurations can be adopted to meet the power demands of miniaturized electronic devices [109–111]. (3) Long-term biocompatibility tests in a systematic manner. For clinical translation of EBFCs, long-term assessment of material toxicity, tissue inflammatory responses, and device stability in physiological settings is vital.

In conclusion, with the further development of EBFC technology, extensive applications are expected to appear in areas such as early screening of chronic diseases, long-term monitoring of biomarkers, implantable precision therapy, and intelligent wound management.

Funding

The authors gratefully acknowledge financial support from the National Natural Science Foundation of China (22474067), the Taishan Scholar Foundation of Shandong Province (tstp20230623 and tsqn202408164), the Natural Science Foundation of Shandong Province (ZR2024QB183), the National Key R&D Program of China-"Intergovernmental International Cooperation on Science and Technology Innovation" Key Special Project (No. 2024YFE0104100), the Open Project of Shandong Provincial Key Laboratory for Tumor Imaging Equipment Development and Tumor Diagnosis & Treatment Integration Technology (2025SHFXTD001), and the open funds of the State Key Laboratory of Chemo and Biosensing (Hunan University).

Acknowledgments

Y.L. and S.Y. contributed equally. All authors discussed the results and approved the manuscript.

Conflicts of Interest

The authors declare no conflict of interest. Given the role as Editorial Board Member, Sai Bi had no involvement in the peer review of this paper and had no access to information regarding its peer-review process. Full responsibility for the editorial process of this paper was delegated to another editor of the journal.

Use of AI and AI-Assisted Technologies

No AI tools were utilized for this paper.

References

1. Wang, X.; Ding, Q.; Groleau, R.R.; et al. Fluorescent probes for disease diagnosis. *Chem. Rev.* **2024**, *124*, 7106–7164.
2. Ma, B.; Shi, J.; Zhang, Y.; et al. Enzymatically activatable polymers for disease diagnosis and treatment. *Adv. Mater.* **2024**, *36*, 2306358.
3. Teixeira Do Nascimento, A.; Stoddart, P.R.; Goris, T.; et al. Stimuli-responsive materials for biomedical applications. *Adv. Mater.* **2025**, *37*, e07559.
4. Wen, D.; Eychmüller, A. Enzymatic biofuel cells on porous nanostructures. *Small* **2016**, *12*, 4649–4661.
5. Schröder, U. From *in vitro* to *in vivo*-biofuel cells are maturing. *Angew. Chem. Int. Ed.* **2012**, *51*, 7370–7372.
6. Zhang, Z.; Zhu, C.; Liang, Y.; et al. Humidity-resistant Pt/$CrVN_2$ fuel cell sensor for H_2S biomarker detection. *ACS Sens.* **2025**, *10*, 4744–4752.
7. Halámková, L.; Halámek, J.; Bocharova, V.; et al. Implanted biofuel cell operating in a living snail. *J. Am. Chem. Soc.* **2012**, *134*, 5040–5043.
8. Choi, E.; Kim, J.H.; Kim, S.H.; et al. Micro-corrugated hydrogel electrodes for high-performance biofuel cells via capillary force and ligand exchange-induced metal nanoparticle assembly. *Small* **2026**, *22*, e12318.

9. Zhong, L.; Tang, L.; Yang, S.; et al. Stretchable liquid metal-based metal-polymer conductors for fully screen-printed biofuel cells. *Anal. Chem.* **2022**, *94*, 16738–16745.
10. Lee, J.; Han, S.; Kwon, Y. Self-charging hybrid energy devices collaborated with enzymatic biofuel cells and supercapacitors. *Chem. Eng. J.* **2024**, *487*, 150557.
11. Huang, W.; Zulkifli, M.Y.B.; Chai, M.; et al. Recent advances in enzymatic biofuel cells enabled by innovative materials and techniques. *Exploration* **2023**, *3*, 20220145.
12. Luo, X.; Li, S.; Wu, Y.; et al. Hybrid enzymatic and nanozymatic biofuel cells for wearable and implantable biosensors. *Trends Anal. Chem.* **2025**, *185*, 118169.
13. Cheng, J.; Han, Y.; Deng, L.; et al. Carbon nanotube-bilirubin oxidase bioconjugate as a new biofuel cell label for self-powered immunosensor. *Anal. Chem.* **2014**, *86*, 11782–11788.
14. Xiao, X.; Xia, H.-Q.; Wu, R.; et al. Tackling the challenges of enzymatic (bio)fuel cells. *Chem. Rev.* **2019**, *119*, 9509–9558.
15. Ji, C.; Hou, J.; Wang, K.; et al. Single-enzyme biofuel cells. *Angew. Chem. Int. Ed.* **2017**, *56*, 9762–9766.
16. Kwon, C.H.; Ko, Y.; Shin, D.; et al. High-power hybrid biofuel cells using layer-by-layer assembled glucose oxidase-coated metallic cotton fibers. *Nat. Commun.* **2018**, *9*, 4479.
17. Kausaite-Minkstimiene, A.; Kaminskas, A.; Ramanaviciene, A. Development of a membraneless single-enzyme biofuel cell powered by glucose. *Biosens. Bioelectron.* **2022**, *216*, 114657.
18. Xiao, X. The direct use of enzymatic biofuel cells as functional bioelectronics. *eScience* **2022**, *2*, 1–9.
19. Luo, X.; Luo, Z.; Li, S.; et al. Nanozymatic biofuel cell-enabled self-powered sensing system for a sensitive immunoassay. *Anal. Chem.* **2023**, *95*, 12306–12312.
20. Xu, J.; Luo, X.; Chen, H.; et al. Machine learning-aided intelligent monitoring of multivariate miRNA biomarkers using bipolar self-powered sensors. *ACS Nano* **2025**, *19*, 8812–8825.
21. Chen, Y.; Wan, X.; Li, G.; et al. Metal hydrogel-based integrated wearable biofuel cell for self-powered epidermal sweat biomarker monitoring. *Adv. Funct. Mater.* **2024**, *34*, 2404329.
22. Lei, W.; Zhang, S.; Shu, J.; et al. Self-powered glucose biosensor based on non-enzymatic biofuel cells by Au nanocluster/Pd nanocube heterostructure and Fe_3C@C-Fe single-atom catalyst. *Small* **2025**, *21*, 2410326.
23. Maity, D.; Guha Ray, P.; Buchmann, P.; et al. Blood-glucose-powered metabolic fuel cell for self-sufficient bioelectronics. *Adv. Mater.* **2023**, *35*, 2300890.
24. Yimamumaimaiti, T.; Lu, X.; Zhang, J.-R.; et al. Efficient blood-toleration enzymatic biofuel cell via in situ protection of an enzyme catalyst. *ACS Appl. Mater. Interfaces* **2020**, *12*, 41429–41436.
25. Wang, C.; Lei, Y.; Xing, Z.; et al. Channel-splitting photoassisted enzyme biofuel cells: A high-confluent and self-powered platform for electrochemistry-photoelectrochemistry-coupled ratiometric bioassays. *Anal. Chem.* **2025**, *97*, 24187–24195.
26. Trifonov, A.; Stemmer, A.; Tel-Vered, R. Power generation by selective self-assembly of biocatalysts. *ACS Nano* **2019**, *13*, 8630–8638.
27. Yahiro, A.T.; Lee, S.M.; Kimble, D.O. Bioelectrochemistry. I. Enzyme utilizing bio-fuel cell studies. *Biochim. Biophys. Acta* **1964**, *88*, 375–383.
28. Zebda, A.; Gondran, C.; Le Goff, A.; et al. Mediatorless high-power glucose biofuel cells based on compressed carbon nanotube-enzyme electrodes. *Nat. Commun.* **2011**, *2*, 370.
29. Jia, W.; Valdés-Ramírez, G.; Bandodkar, A.J.; et al. Epidermal biofuel cells: Energy harvesting from human perspiration. *Angew. Chem. Int. Ed.* **2013**, *52*, 7233–7236.
30. Ó Conghaile, P.; Falk, M.; Macaodha, D.; et al. Fully enzymatic membraneless glucose|oxygen fuel cell that provides 0.275 mA cm^{-2} in 5 mM glucose, operates in human physiological solutions, and powers transmission of sensing data. *Anal. Chem.* **2016**, *88*, 2156–2163.
31. Gai, P.; Kong, X.; Pu, L.; et al. Biofuel cell-driven robust electrochemiluminescence biosensing platform. *Anal. Chem.* **2021**, *93*, 11745–11750.
32. Falk, M.; Andoralov, V.; Silow, M.; et al. Miniature biofuel cell as a potential power source for glucose-sensing contact lenses. *Anal. Chem.* **2013**, *85*, 6342–6348.
33. Grattieri, M.; Minteer, S.D. Self-powered biosensors. *ACS Sens.* **2018**, *3*, 44–53.
34. Zhao, C.-E.; Gai, P.; Song, R.; et al. Nanostructured material-based biofuel cells: Recent advances and future prospects. *Chem. Soc. Rev.* **2017**, *46*, 1545–1564.
35. Huang, X.; Zhang, L.; Zhang, Z.; et al. Wearable biofuel cells based on the classification of enzyme for high power outputs and lifetimes. *Biosens. Bioelectron.* **2019**, *124*, 40–52.
36. Zhao, M.; Gao, Y.; Sun, J.; et al. Mediatorless glucose biosensor and direct electron transfer type glucose/air biofuel cell enabled with carbon nanodots. *Anal. Chem.* **2015**, *87*, 2615–2622.

37. Ravenna, Y.; Xia, L.; Gun, J.; et al. Biocomposite based on reduced graphene oxide film modified with phenothiazone and flavin adenine dinucleotide-dependent glucose dehydrogenase for glucose sensing and biofuel cell applications. *Anal. Chem.* **2015**, *87*, 9567–9571.
38. Pinyou, P.; Blay, V.; Muresan, L.M.; et al. Enzyme-modified electrodes for biosensors and biofuel cells. *Mater. Horiz.* **2019**, *6*, 1336–1358.
39. Yu, W.; Jin, D.; Zhang, Y.; et al. Provoking tumor disulfidptosis by single-atom nanozyme via regulating cellular energy supply and reducing power. *Nat. Commun.* **2025**, *16*, 4877.
40. Wang, D.; Yan, L.; Ma, X.; et al. Ultrasound promotes enzymatic reactions by acting on different targets: Enzymes, substrates and enzymatic reaction systems. *Int. J. Biol. Macromol.* **2018**, *119*, 453–461.
41. Blaik, R.A.; Lan, E.; Huang, Y.; et al. Gold-coated M13 bacteriophage as a template for glucose oxidase biofuel cells with direct electron transfer. *ACS Nano* **2016**, *10*, 324–332.
42. Zion, N.; Friedman, A.; Levy, N.; et al. Bioinspired electrocatalysis of oxygen reduction reaction in fuel cells using molecular catalysts. *Adv. Mater.* **2018**, *30*, 1800406.
43. Ma, C.L.; Wu, R.R.; Huang, R.; et al. Directed evolution of a 6-phosphogluconate dehydrogenase for operating an enzymatic fuel cell at lowered anodic pHs. *J. Electroanal. Chem.* **2019**, *851*, 113444.
44. Vornholt, T.; Leiss-Maier, F.; Jeong, W.J.; et al. Artificial metalloenzymes. *Nat. Rev. Methods Primers* **2024**, *4*, 78.
45. Wu, T.; Chen, X.; Fei, Y.; et al. Artificial metalloenzyme assembly in cellular compartments for enhanced catalysis. *Nat. Chem. Biol.* **2025**, *21*, 779–789.
46. Wang, J.; Ma, J.; Cheng, H. Nanomaterials-based enzymatic biofuel cells for wearable and implantable bioelectronics. *Front. Energy* **2025**, *19*, 283–299.
47. Wu, H.; Zhang, Y.; Kjøniksen, A.L.; et al. Wearable biofuel cells: Advances from fabrication to application. *Adv. Funct. Mater.* **2021**, *31*, 2103976.
48. Gallaway, J.W.; Calabrese Barton, S.A. Kinetics of redox polymer-mediated enzyme electrodes. *J. Am. Chem. Soc.* **2008**, *130*, 8527–8536.
49. Mano, N.; De Poulpiquet, A. O_2 reduction in enzymatic biofuel cells. *Chem. Rev.* **2018**, *118*, 2392–2468.
50. Deng, W.; Liu, S.; Mei, Y.; et al. Self-powered detection of T4 polynucleotide kinase activity based on DNA structure transformation-modulated direct electron transfer of bilirubin oxidase. *Talanta* **2026**, *297*, 128686.
51. Hou, C.; Yang, D.; Liang, B.; et al. Enhanced performance of a glucose/O_2 biofuel cell assembled with laccase-covalently immobilized three-dimensional macroporous gold film-based biocathode and bacterial surface displayed glucose dehydrogenase-based bioanode. *Anal. Chem.* **2014**, *86*, 6057–6063.
52. Babanova, S.; Matanovic, I.; Chavez, M.S.; et al. Role of quinones in electron transfer of PQQ-glucose dehydrogenase anodes-mediation or orientation effect. *J. Am. Chem. Soc.* **2015**, *137*, 7754–7762.
53. Zhang, J.L.; Wang, Y.H.; Huang, K.; et al. Enzyme-based biofuel cells for biosensors and *in vivo* power supply. *Nano Energy* **2021**, *84*, 105853.
54. Ruth, J.C.; Spormann, A.M. Enzyme electrochemistry for industrial energy applications-a perspective on future areas of focus. *ACS Catal.* **2021**, *11*, 11654–11668.
55. Muguruma, H.; Kase, Y.; Uehara, H. Nanothin ferrocene film plasma polymerized over physisorbed glucose oxidase: High-throughput fabrication of bioelectronic devices without chemical modifications. *Anal. Chem.* **2005**, *77*, 6557–6562.
56. Rodrigues, R.C.; Berenguer-Murcia, A.; Carballares, D.; et al. Stabilization of enzymes via immobilization: Multipoint covalent attachment and other stabilization strategies. *Biotechnol. Adv.* **2021**, *52*, 107821.
57. Prabhakar, T.; Giaretta, J.; Zulli, R.; et al. Covalent immobilization: A review from an enzyme perspective. *Chem. Eng. J.* **2024**, *503*, 158054.
58. Park, S.; Kim, G.; Seo, J.; et al. Ultrasensitive protease sensors using selective affinity binding, selective proteolytic reaction, and proximity-dependent electrochemical reaction. *Anal. Chem.* **2016**, *88*, 11995–12000.
59. Zhang, R.; Yan, X.; Fan, K. Nanozymes inspired by natural enzymes. *Acc. Mater. Res.* **2021**, *2*, 534–547.
60. Hadt, R.G.; Gorelsky, S.I.; Solomon, E.I. Anisotropic covalency contributions to superexchange pathways in type one copper active sites. *J. Am. Chem. Soc.* **2014**, *136*, 15034–15045.
61. Gong, H.; Meng, Y.; Sun, Y.; et al. Design of a programmable and recyclable protein scaffolding material with geometrically precise enzyme patterning for improved cascade catalysis. *Adv. Funct. Mater.* **2026**, *36*, e14761.
62. Ye, J.; Lu, J.; Wen, D. Engineering carbon nanomaterials toward high-efficiency bioelectrocatalysis for enzymatic biofuel cells: A review. *Mater. Chem. Front.* **2023**, *7*, 5806–5825.
63. Zhou, J.; Liu, C.; Yu, H.; et al. Research progresses and application of biofuel cells based on immobilized enzymes. *Appl. Sci.* **2023**, *13*, 5917.
64. Katz, E.; Bückmann, A.F.; Willner, I. Self-powered enzyme-based biosensors. *J. Am. Chem. Soc.* **2001**, *123*, 10752–10753.
65. Hou, C.; Fan, S.; Lang, Q.; et al. Biofuel cell based self-powered sensing platform for l-cysteine detection. *Anal. Chem.* **2015**, *87*, 3382–3387.

66. Lv, P.; Zhou, H.; Mensah, A.; et al. A highly flexible self-powered biosensor for glucose detection by epitaxial deposition of gold nanoparticles on conductive bacterial cellulose. *Chem. Eng. J.* **2018**, *351*, 177–188.
67. Zhang, J.; Liu, J.; Su, H.; et al. A wearable self-powered biosensor system integrated with diaper for detecting the urine glucose of diabetic patients. *Sens. Actuators B* **2021**, *341*, 130046.
68. Lee, I.; Sode, T.; Loew, N.; et al. Continuous operation of an ultra-low-power microcontroller using glucose as the sole energy source. *Biosens. Bioelectron.* **2017**, *93*, 335–339.
69. Gonzalez-Solino, C.; Bernalte, E.; Bayona Royo, C.; et al. Self-powered detection of glucose by enzymatic glucose/oxygen fuel cells on printed circuit boards. *ACS Appl. Mater. Interfaces* **2021**, *13*, 26704–26711.
70. Guo, Y.; Shang, Y.; Han, X.; et al. Carbon-nanotube synergized robust enzymatic-fuel-cell in gel microneedle for self-powered monitoring and forecasting. *Adv. Mater.* **2025**, *37*, 2313837.
71. Li, J.; Tan, S.; Kooger, R.; et al. MicroRNAs as novel biological targets for detection and regulation. *Chem. Soc. Rev.* **2013**, *42*, 506–517.
72. Liu, H.; Fu, Z.; Han, Y.; et al. Conditionally activatable chimeras for tumor-specific membrane protein degradation. *J. Am. Chem. Soc.* **2024**, *146*, 32933–32941.
73. Wu, D.; Yu, Z.; Qin, J.; et al. A bimetallic nanozyme synergistic effect-driven enzyme cascade nanoreactor for instant immunoassay. *Anal. Chem.* **2025**, *97*, 10947–10954.
74. Yan, Y.; Guo, L.; Geng, H.; et al. Hierarchical porous metal-organic framework as biocatalytic microreactor for enzymatic biofuel cell-based self-powered biosensing of microRNA integrated with cascade signal amplification. *Small* **2023**, *19*, 2301654.
75. Gai, P.; Gu, C.; Hou, T.; et al. Integration of biofuel cell-based self-powered biosensing and homogeneous electrochemical strategy for ultrasensitive and easy-to-use bioassays of microRNA. *ACS Appl. Mater. Interfaces* **2018**, *10*, 9325–9331.
76. Song, Y.; Ya, Y.; Cen, X.; et al. Multiple signal amplification strategy induced by biomarkers of lung cancer: A self-powered biosensing platform adapted for smartphones. *Int. J. Biol. Macromol.* **2024**, *264*, 130661.
77. Wang, F.; Cai, R.; Tan, W. Self-powered biosensor for a highly efficient and ultrasensitive dual-biomarker assay. *Anal. Chem.* **2023**, *95*, 6046–6052.
78. Xu, J.; Li, Y.; Wang, F.; et al. A smartphone-mediated "all-in-one" biosensing chip for visual and value-assisted detection. *Anal. Chem.* **2024**, *96*, 15780–15788.
79. Jin, Y.; Wu, Z.; Li, L.; et al. Zinc-air battery-based self-powered sensor with high output power for ultrasensitive microRNA let-7a detection in cancer cells. *Anal. Chem.* **2022**, *94*, 14368–14376.
80. Gai, P.; Song, R.; Zhu, C.; et al. Ultrasensitive self-powered cytosensors based on exogenous redox-free enzyme biofuel cell as point-of-care tools for early cancer diagnosis. *Chem. Commun.* **2015**, *51*, 16763–16766.
81. Gai, P.-P.; Ji, Y.-S.; Wang, W.-J.; et al. Ultrasensitive self-powered cytosensor. *Nano Energy* **2016**, *19*, 541–549.
82. Yimamumaimaiti, T.; Su, Q.; Song, R.-B.; et al. Damage-free and time-saving platform integrated by a flow membrane separation device and a dual-target biofuel cell-based biosensor for continuous sorting and detection of exosomes and host cells in human serum. *Anal. Chem.* **2022**, *94*, 7722–7730.
83. Men, J.; Lv, S.; Wang, Y.; et al. Stimuli-responsive barcode probe-mediated self-powered biosensor enables dual-signal amplification for ultrasensitive detection of circulating tumor cells. *Anal. Chem.* **2025**, *97*, 8056–8064.
84. Tan, R.; Zhang, S.; Jia, W.; et al. Exercise-induced stimulation of self-powered nanofibers for aspirin/lysine delivery in the prevention of denervated muscle atrophy. *ACS Nano* **2025**, *19*, 31481–31495.
85. Yao, S.; Zheng, M.; Wang, Z.; et al. Self-powered, implantable, and wirelessly controlled NO generation system for intracranial neuroglioma therapy. *Adv. Mater.* **2022**, *34*, 2205881.
86. Song, P.; Kuang, S.; Panwar, N.; et al. A self-powered implantable drug-delivery system using biokinetic energy. *Adv. Mater.* **2017**, *29*, 1605668.
87. Ogawa, Y.; Kato, K.; Miyake, T.; et al. Organic transdermal iontophoresis patch with built-in biofuel cell. *Adv. Healthc. Mater.* **2015**, *4*, 506–510.
88. Xiao, X.; McGourty, K.D.; Magner, E. Enzymatic biofuel cells for self-powered, controlled drug release. *J. Am. Chem. Soc.* **2020**, *142*, 11602–11609.
89. Li, Z.; Wu, R.; Chen, K.; et al. Enzymatic biofuel cell-powered iontophoretic facial mask for enhanced transdermal drug delivery. *Biosens. Bioelectron.* **2022**, *223*, 115019.
90. Zhang, H.; Pan, Y.; Hou, Y.; et al. Smart physical-based transdermal drug delivery system: Towards intelligence and controlled release. *Small* **2024**, *20*, 2306944.
91. Amjadi, M.; Sheykhansari, S.; Nelson, B.J.; et al. Recent advances in wearable transdermal delivery systems. *Adv. Mater.* **2018**, *30*, 1704530.
92. Guan, S.; Wang, J.; Yang, Y.; et al. Microneedle-based biofuel cell with MXene/CNT hybrid bioanode: Fundamental and biomedical application. *Adv. Sci.* **2025**, *12*, e16229.
93. Luo, R.; Dai, J.; Zhang, J.; et al. Accelerated skin wound healing by electrical stimulation. *Adv. Healthc. Mater.* **2021**, *10*, 2100557.

94. Lee, J.H.; Jeon, W.-Y.; Kim, H.-H.; et al. Electrical stimulation by enzymatic biofuel cell to promote proliferation, migration and differentiation of muscle precursor cells. *Biomaterials* **2015**, *53*, 358–369.
95. Kai, H.; Yamauchi, T.; Ogawa, Y.; et al. Accelerated wound healing on skin by electrical stimulation with a bioelectric plaster. *Adv. Healthc. Mater.* **2017**, *6*, 1700465.
96. Shin, T.E.; Park, J.W.; Jeon, W.-Y.; et al. Motility enhancement of human spermatozoa using electrical stimulation in the nano-ampere range with enzymatic biofuel cells. *PLoS ONE* **2020**, *15*, e0228097.
97. Deng, H.; Xiang, Z.; Yan, K.; et al. Self-powered enzymatic biofuel cell for synergistic therapy and real-time monitoring of diabetic wounds. *Adv. Healthc. Mater.* **2026**, *15*, e05909.
98. Wang, Y.; Hai, X.; Yan, Y.; et al. Self-powered biosensor-based multifunctional platform for detection and in situ elimination of bacteria. *Adv. Funct. Mater.* **2025**, *35*, 2420480.
99. Geng, H.; Zhi, S.; Zhou, X.; et al. Self-powered engineering of cell membrane receptors to on-demand regulate cellular behaviors. *Nano Lett.* **2024**, *24*, 7895–7902.
100. Liu, R.; Wang, Z.L.; Fukuda, K.; et al. Flexible self-charging power sources. *Nat. Rev. Mater.* **2022**, *7*, 870–886.
101. Moonla, C.; Reynoso, M.; Chang, A.-Y.; et al. Microneedle-based multiplexed monitoring of diabetes biomarkers: Capabilities beyond glucose toward closed-loop theranostic systems. *ACS Sens.* **2025**, *10*, 5363–5379.
102. Lin, Z.; Wu, Y.; Wang, Y.; et al. Flexible patterned fuel cell patches stimulate nerve and myocardium restoration. *Adv. Mater.* **2025**, *37*, 2416410.
103. Wang, C.; He, G.; Zhao, H.; et al. Enhancing deep-seated melanoma therapy through wearable self-powered microneedle patch. *Adv. Mater.* **2024**, *36*, 2311246.
104. Zhou, M.; Zhou, N.; Kuralay, F.; et al. A self-powered "sense-act-treat" system that is based on a biofuel cell and controlled by boolean logic. *Angew. Chem. Int. Ed.* **2012**, *51*, 2686–2689.
105. Wang, L.; Shao, H.; Lu, X.; et al. A glucose/O_2 fuel cell-based self-powered biosensor for probing a drug delivery model with self-diagnosis and self-evaluation. *Chem. Sci.* **2018**, *9*, 8482–8491.
106. Demkiv, O.; Stasyuk, N.; Gayda, G.; et al. Biofuel cells based on oxidoreductases and electroactive nanomaterials: Development and characterization. *Biosensors* **2025**, *15*, 249.
107. Trifonov, A.; Herkendell, K.; Tel-Vered, R.; et al. Enzyme-capped relay-functionalized mesoporous carbon nanoparticles: Effective bioelectrocatalytic matrices for sensing and biofuel cell applications. *ACS Nano* **2013**, *7*, 11358–11368.
108. Koga, H.; Nagashima, K.; Suematsu, K.; et al. Nanocellulose paper semiconductor with a 3D network structure and its nano-micro-macro trans-scale design. *ACS Nano* **2022**, *16*, 8630–8640.
109. Fredj, Z.; Rong, G.; Sawan, M. Recent advances in enzymatic biofuel cells to power up wearable and implantable biosensors. *Biosensors* **2025**, *15*, 218.
110. Dai, H.; Chen, G.; Mu, J.; et al. Universal electrode based on ferredoxin-$NADP^+$ oxidoreductase enables enzymatic biofuel cells with broad substrate spectrum. *Biotechnol. J.* **2025**, *20*, e70090.
111. Riedel, M.; Höfs, S.; Ruff, A.; et al. A tandem solar biofuel cell: Harnessing energy from light and biofuels. *Angew. Chem. Int. Ed.* **2020**, *60*, 2078–2083.